

## Hierarchical Crystalline Superstructures of Conducting Polymers with Homohelicity

Yong Yan,<sup>[a, c]</sup> Yajie Zhang,<sup>[b, c]</sup> Wenping Hu,<sup>[b]</sup> and Zhixiang Wei\*<sup>[a]</sup>

Inspired by the helicity of biological materials, there is increasing interest in producing helical synthetic materials, such as helical polymers, as well as their supramolecular assemblies.<sup>[1]</sup> In particular, chiral functional materials with electrical, optical, and magnetic properties are highly desired in the development of multifunctional materials.<sup>[2]</sup> By delicately controlling steric hindrance and noncovalent interactions, stereoselective synthesis of enantiomeric polymers and their assemblies were realized.<sup>[3]</sup> On the other hand, synergetic properties are reported by the combination of chirality with functional properties, which have potential applications in chiral recognition and separation, chiral optical switch and memory, and chiral sensors.<sup>[4]</sup>

As a typical conducting polymer with excellent physical properties, various polyaniline (PANI) nanostructures have been reported by an in situ polymerization process.<sup>[5]</sup> PANI, with predominately one-handed helical conformation, and even their helical nanofibers were then prepared by the induction of enantiomeric acidic dopants.<sup>[6]</sup> However, all PANI nanofibers were entangled together, which led to difficulties in characterizing their physical properties. Moreover, compared with the abundant fascinating architectures created by DNAs and peptides,<sup>[7]</sup> helical functional nanostructures with complicated architectures have rarely been prepared, especially those with controlled molecular arrangements.

Herein, we report that hierarchical crystalline superstructures of PANI with homohelicity can be prepared by a self-assembly process. PANI with helical conformations was firstly prepared by the induction of chiral camphorsulfonic acid (CSA) as a dopant, and then helical nanofibers with different dimensions, such as linear, branched, and microribbons composed of aligned nanofibers, were produced by self-assembly. The helical PANI molecules are oriented perpendicular to the long axis of the helical nanofiber, which is quite similar to the arrangement of peptides in their  $\beta$ -sheet assemblies.<sup>[8]</sup>

For the preparation of PANI nanostructures and their superstructures, a small amount of as-prepared helical PANI solution was first diluted with good solvent (mixture of THF/CHCl<sub>3</sub> with a volume ratio of 1/3). Poor solvent, methanol, was then added according to the volume ratio of good solvent to poor solvent ([G]/[P]). PANI helical superstructures with linear, branched, and aligned morphologies were obtained through a self-assembly process by varying [G]/[P] ratio from 0:100 to 50:50 (Figure 1). Linear nanofibers (Figure 1a) were obtained by adding only poor solvent ([G]/[P]=0:100) through a fast aggregation process.

Interestingly, branched helical nanofibers were observed when the [G]/[P] ratio increased to 40:60. Since branched nanostructures were obtained by a slower process than that of linear ones, we suggest that linear PANI nanofibers aggregated together during self-assembly processes. Finally, nanostructures with three, four, and even more branches were all observed in a same sample (Figure 1b and c, and Figure S1 in the Supporting Information). Moreover, the left-handed helical sense of the branches could be clearly observed in the enlarged SEM images (Figure 1d), which indicates that the helical conformation of PANI molecules was expressed in their supramolecular assemblies.

When the [G]/[P] ratio increased to 50:50, microribbons composed of aligned PANI nanofibers were obtained due to an even slower self-assembly process. Tens of nanofibers were aggregated by the connection of numerous junctions, and were all aligned along the same direction to form a microribbon (Figure 1e). The microribbons were also easily

[a] Dr. Y. Yan, Prof. Z. Wei  
National Center for Nanoscience and Technology  
Beijing 100190 (China)  
Fax: (+86)10-6265-6765  
E-mail: weizx@nanoctr.cn

[b] Dr. Y. Zhang, Prof. W. Hu  
Institute of Chemistry, Chinese Academy of Sciences  
Beijing 100190 (China)

[c] Dr. Y. Yan, Dr. Y. Zhang  
Graduate School of Chinese Academy of Sciences  
Beijing 100039 (China)

Supporting information for this article is available on the WWW under <http://dx.doi.org/10.1002/chem.201000999>.

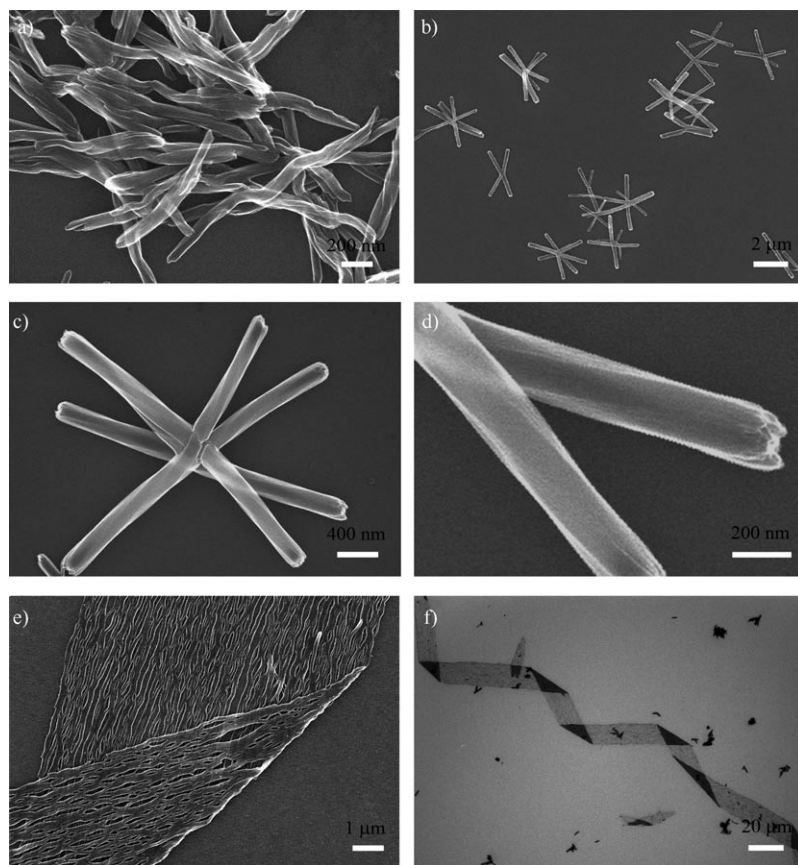


Figure 1. SEM and optical images of linear, branched and aligned PANI helical nanofibers. a) Linear; b) branched helical nanofibers; c) single branched helical nanofibers with seven branches; d) magnified image of the bottom right position in image c), which clearly shows the left-handed helical screws; e) SEM; and f) optical images of aligned helical nanofibers.

observed by using optical microscopy (Figure 1 f), which shows that they are even longer than 100  $\mu\text{m}$ . PANI micro-ribbons had a high tendency for right-handed curving, but homo-handedness is difficult to obtain at present. To the best of our knowledge, microribbons composed of helical nanofibers of functional materials were prepared for the first time, which would be facile for the study of their physical properties. For instance, we constructed the devices based on a single microribbon, and its resistance was measured as 6.3  $\text{M}\Omega$  (Figure S2 in the Supporting Information), from which we calculated its conductivity as about  $0.01 \text{ Scm}^{-1}$ . The conductivity of PANI is lower than PANI films doped with CSA,<sup>[9]</sup> which could be ascribed to partial dedoping as indicated in the UV/Vis absorption spectra.

Subsequently, PANI helical superstructures were characterized by circular dichroism (CD) and UV/Vis spectroscopy (Figure 2). All UV/Vis spectra show a dominant band at around 800 nm, and the solutions at all [G]/[P] ratios are green in color (Figure S3 in the Supporting Information), which indicated that most of the PANI molecules are in a conducting state. However, shoulder peaks at around 600 nm appeared for the PANI superstructures, which are ascribed to the partial dedoping of PANI upon adding methanol. PANI molecules existed in an extended coil conforma-

tion in the solid state, and could be fully redoped by immersion in solutions of CSA (Figure S4 in the Supporting Information). PANI helical nanostructures show a bisignate CD signal with a positive CD peak at around 425 nm and a negative CD peak at about 460 nm (i.e., a split signal with a crossover at ca. 440 nm as shown in Figure 2 a), which is ascribed to the chiral excitonic coupling corresponding to the absorption at about 430 nm in Figure 2 b.<sup>[9]</sup> The negative signal at around 625 nm should be ascribed to dipolarons corresponding to the absorption at around 650 nm. The strongest CD intensity indicated the relatively intensified screws at all [G]/[P] ratios. L-CSA-induced PANIs showed mirror images in CD spectra to those of D-CSA-induced PANIs, whereas their UV/Vis spectra were almost identical (Figure 2 c and d), which further proved that helical PANIs were induced by chiral dopant.

However, the CD spectra of D-CSA-induced helical PANI in good solvent showed a bisignate CD signal with a negative CD peak at around 400 nm and a positive CD peak at around 450 nm, which corresponded to the right-handed helix of the PANI conformation.

The inversion of the CD signal of the nanostructure to that of the solution indicates that PANI molecules arranged normal to the nanofiber direction,<sup>[10]</sup> which will be further proved as described below.

To further investigate superstructures of PANI, TEM measurements were carried out for branched nanostructures. As described above, branched helical nanofibers with clear left-handed screw directions were observed by SEM (Figure 1 c and d and Figure S1 in the Supporting Information) with a high  $p/d$  ratio (the ratio between screw pitch  $p$  and diameter  $d$ ). A TEM image at a low magnification (Figure 3 a) clearly showed the junctions and helical branches of branched nanostructures. A high-magnification image of one branch (Figure 3 c) showed very clear dark helical strips of the nanofiber, from which we can get its pitch size  $p = 2.2 \mu\text{m}$ , diameter  $d = 290 \text{ nm}$ , and screw angle  $\Phi = 7.6^\circ$ .

Selected-area electron diffraction (SAED) and X-ray powder diffraction (XRD) patterns, shown in Figure 3 b and d, respectively, reveal that PANI molecules have long-range orders in the nanostructures. Diffused reflections corresponding to a  $d$  spacing of approximately 3.5  $\text{\AA}$  in the

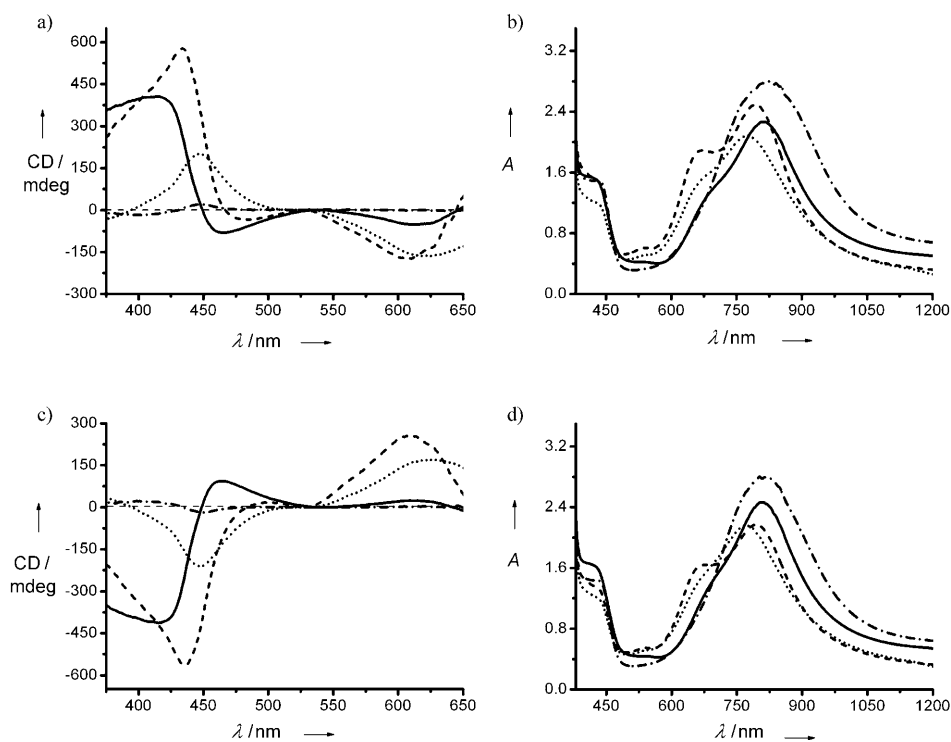


Figure 2. CD (a) and UV/Vis (b) spectra of as-prepared polyaniline, helical nanostructures induced by D-CSA at different volume ratios of [G]/[P]. CD (c) and UV/Vis (d) spectra of PANIs induced by L-CSA at different volume ratios of [G]/[P]. —: 0:100, ---: 40:60, ·····: 50:50, - - - -: 100:0 [G]/[P].

SAED pattern resulted from a (040) reflection of a planar PANI molecule  $\pi$ - $\pi$  stacking along the long axis of the fiber.<sup>[11]</sup> Rather sharp reflections corresponding to a  $d$  spacing of about 6.1 Å from the (100) reflection could be ascribed to the arrangement of CSA molecules sitting between neighboring PANI chains. The strong reflection in the XRD pattern with a  $d$  value = 28 Å from the (001) reflection was overwhelmed by the intense transmission beam in SAED pattern, but the sharp reflections in the SAED pattern corresponding to a  $d$  spacing of 10 Å might belong to the (003) reflection of the same diffraction family.

Based on the SAED and XRD analysis, a formation mechanism for PANI helical nanofibers was proposed as illustrated in Figure 3 f. PANI molecules were doped with enantiomeric CSA to form a complex (here we used D-CSA as an example, and the difference of the PANI in solution and in the solid state is illustrated in Figure S5 in the Supporting Information). Due to the steric hindrance of CSA, rectangular-like PANI molecules were twisted in the solution. This twist was amplified by  $\pi$ - $\pi$  stacking of conjugated chains during the self-assembly process, and finally a helical nanofibers was obtained. The cell parameters of the PANI nanofibers in this model is quite similar with that of the oligoaniline-surfactant complexes.<sup>[12]</sup>

The orientation of PANI molecules in nanofibers could be further proved by polarized Raman spectroscopy.<sup>[13]</sup> Figure 3 e shows the results of single helical nanofibers for both polarization geometries. The depolarization ratio ( $\rho_{\text{iso}}$ ) of Raman bands was expressed by  $I_{\text{normal}}/I_{\text{parallel}}$ , in which  $I_{\text{normal}}$

and  $I_{\text{parallel}}$  are the scattering intensities, for which the incident beam is normal or parallel to the long axis of the nanofiber, respectively. Both directions show typical Raman scattering spectra of PANI with a C=C quinoid stretching at 1595  $\text{cm}^{-1}$ , a C=N quinoid stretching at 1470–1495  $\text{cm}^{-1}$ , a C-N<sup>+</sup> stretching at 1339  $\text{cm}^{-1}$ , a C-N benzenoid stretching at 1222  $\text{cm}^{-1}$ , and a C-H benzenoid or quinoid stretching at around 1160  $\text{cm}^{-1}$ .<sup>[14]</sup> However, the scattering intensity in normal direction is much stronger than that in parallel direction with  $\rho_{\text{iso}} \approx 3$ , which means that the packing direction of helical PANI in branched helical nanofibers is normal to the direction of nanofibers as illustrated in Figure 3 f.

In fact, this packing means is very common in biological species, such as the  $\beta$ -pleated sheet of proteins.<sup>[8]</sup> In a  $\beta$ -pleated

sheet, the basic unit of the chiral peptide is normal to the direction of the aggregates, which is very similar to the helical PANI in branched helical nanofibers. Therefore, the building block of helical PANI is quite similar to random-coiled peptides in solution, and the helical nanofiber is an analogue of  $\beta$ -sheet assemblies of peptides. This helical nanofibers composed of helical PANI would not only help people to understand the self-assembly behavior of protein, but also put the conducting function in the assemblies of  $\beta$ -sheet analogues, which lead to new physical properties for self-assembled superstructures.

In summary, helical PANI was induced by a chiral dopant and further self-assembled into different hierarchical helical superstructures with different [G]/[P] ratios. As the [G]/[P] ratios increased, linear, branched, and aligned helical nanofibers were successively obtained by control their aggregation behavior. Structural studies indicated that helical PANI molecules are arranged normal to the long axis of nanofibers, which is very similar to that of peptide  $\beta$ -sheet assemblies. This study will further inspire studies on self-assembling analogues of bimolecular assemblies using other functional molecules.

## Experimental Section

The synthesis of helical polyaniline; the preparation of linear, branched, and aligned helical nanofibers; morphology; and structure characterizations are given in the Supporting Information.

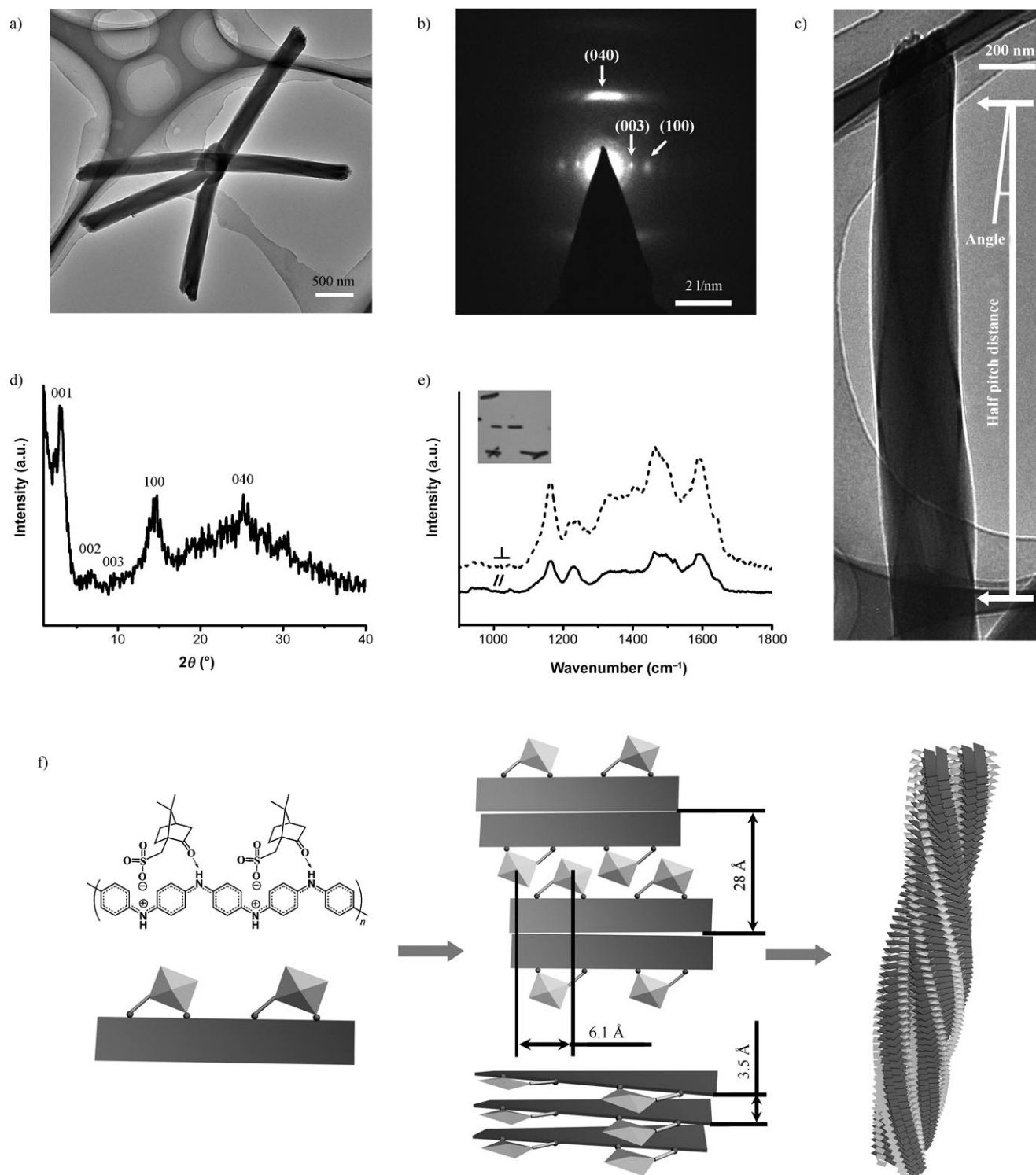


Figure 3. a) TEM image of branched helical nanofibers induced by D-CSA dopant at low magnification. b) The SAED patterns corresponding to the single nanofiber in the TEM image of c). d) XRD pattern of the PANI powder. e) Polarized Raman scattering spectra of PANI helical nanofibers, the insert is the optical image of the nanofiber. —: parallel, ----: vertical. f) Schematic illustration of the formation mechanism of the helical nanofiber. The helical conformation of PANI was induced by enantiomeric CSA as the dopant, and helical PANIs further self-assembled into helical nanofibers through  $\pi$ - $\pi$  interactions of PANI and hydrophobic interactions of CSA. PANI molecules are normal to the long axis of the nanofiber as illustrated.

## Acknowledgements

We acknowledge the financial support of the National Natural Science Foundation of China (grants 20604008, 20974029), The Ministry of Science and Technology of China (2006CB932100, 2009CB930400), and Chinese Academy of Sciences (KJ921-A1-101-1). We thank Prof. M. He, National Center for Nanoscience and Technology of China, for helpful discussions on SAED and XRD results.

**Keywords:** chirality • crystallinity • polyanilines • self-assembly • superstructures

- [1] a) J. J. L. M. Cornelissen, M. Fischer, N. A. J. M. Sommerdijk, R. J. M. Nolte, *Science* **1998**, *280*, 1427–1430; b) E. Yashima, K. Maeda, Y. Furusho, *Acc. Chem. Res.* **2008**, *41*, 1166–1180; c) K. P. R. Nilsson, J. Rydberg, L. Baltzer, O. Inganäs, *Proc. Natl. Acad. Sci. USA* **2004**, *101*, 11197–11202; d) L. C. Palmer, S. I. Stupp, *Acc. Chem. Res.* **2008**, *41*, 1674–1684; e) H. Ito, Y. Furusho, T. Hasegawa, E. Yashima, *J. Am. Chem. Soc.* **2008**, *130*, 14008–14015.
- [2] a) F. J. M. Hoeben, P. Jonkheijm, E. W. Meijer, A. P. H. J. Schenning, *Chem. Rev.* **2005**, *105*, 1491–1546; b) T. Kaneko, H. Katagiri, Y. Umeda, T. Namikoshi, E. Marwanta, M. Teraguchi, T. Aoki, *Polyhedron* **2009**, *28*, 1927–1929; c) N. Avarvari, J. D. Wallis, *J. Mater. Chem.* **2009**, *19*, 4061–4076.
- [3] a) P. Jonkheijm, P. van der Schoot, A. P. H. J. Schenning, E. W. Meijer, *Science* **2006**, *313*, 80–83; b) R. S. Johnson, T. Yamazaki, A. Kovalenko, H. Fenniri, *J. Am. Chem. Soc.* **2007**, *129*, 5735–5743; c) C. Dolain, H. Jiang, J. Léger, P. Guionneau, I. Huc, *J. Am. Chem. Soc.* **2005**, *127*, 12943–12951; d) Y. Yan, K. Deng, Z. Yu, Z. Wei, *Angew. Chem.* **2009**, *121*, 2037–2040; *Angew. Chem. Int. Ed.* **2009**, *48*, 2003–2006.
- [4] a) J. Huang, V. M. Egan, H. Guo, J. Y. Yoon, A. L. Briseno, I. E. Rauda, R. L. Garrell, C. M. Knobler, F. Zhou, R. B. Kaner, *Adv. Mater.* **2003**, *15*, 1158–1161; b) A. Ohira, K. Okoshi, M. Fujiki, M. Kunitake, M. Naito, T. Hagihara, *Adv. Mater.* **2004**, *16*, 1645–1650; c) L. Torsi, G. M. Farinola, F. Marinelli, M. C. Tanese, O. H. Omar, L. Valli, F. Babudri, F. Palmisano, P. G. Zamboni, F. Naso, *Nat. Mater.* **2008**, *7*, 412–417.
- [5] a) J. Huang, R. B. Kaner, *J. Am. Chem. Soc.* **2004**, *126*, 851–855; b) N. Nuraje, K. Su, N. I. Yang, H. Matsui, *ACS Nano* **2008**, *2*, 502–506.
- [6] a) E. E. Havinga, M. M. Bouman, E. W. Meijer, A. Pomp, M. M. J. Simenon, *Synth. Met.* **1994**, *66*, 93–97; b) M. R. Majidi, L. A. P. Kane-Maguire, G. G. Wallace, *Polymer* **1995**, *36*, 3597–3599; c) Y. Yan, Z. Yu, Y. Huang, W. Yuan, Z. Wei, *Adv. Mater.* **2007**, *19*, 3353–3357; d) W. Li, H. Wang, *J. Am. Chem. Soc.* **2004**, *126*, 2278–2279.
- [7] a) F. A. Aldaye, A. L. Palmer, H. F. Sleiman, *Science* **2008**, *321*, 1795–1799; b) J. Sharma, R. Chhabra, A. Cheng, J. Brownell, Y. Liu, H. Yan, *Science* **2009**, *323*, 112–116; c) S. M. Douglas, H. Dietz, T. Liedl, B. Högberg, F. Graf, W. M. Shih, *Nature* **2009**, *459*, 414–418; d) R. Zhang, E. O. McCullum, J. C. Chaput, *J. Am. Chem. Soc.* **2008**, *130*, 5846–5847; e) X. Zhao, S. Zhang, *Macromol. Biosci.* **2007**, *7*, 13–22; Zhao, S. Zhang, *Macromol. Biosci.* **2007**, *7*, 13–22; f) H. Dietz, S. M. Douglas, W. M. Shih, *Science* **2009**, *325*, 725–730.
- [8] a) I. W. Hamley, *Angew. Chem.* **2007**, *119*, 8274–8295; *Angew. Chem. Int. Ed.* **2007**, *46*, 8128–8147; b) S. Scanlon, A. Aggeli, *Nano Today* **2008**, *3*, 22–30; c) J. L. Jimenez, E. J. Nettleton, M. Bouchard, C. V. Robinson, C. M. Dobson, H. R. Saibil, *Proc. Natl. Acad. Sci. USA* **2002**, *99*, 9196–9201.
- [9] a) Y. Cao, P. Smith, A. J. Heeger, *Synth. Met.* **1992**, *48*, 91–93; b) A. G. MacDiarmid, A. J. Epstein, *Synth. Met.* **1995**, *69*, 85–92; c) M. R. Majidi, L. A. P. Kane-Maguire, G. G. Wallace, *Polymer* **1995**, *36*, 3597–3599.
- [10] a) J. Tabei, R. Nomura, M. Shiotsuki, F. Sanda, T. Masuda, *Macromol. Chem. Phys.* **2005**, *206*, 323–332; b) W. Peng, M. Motonaga, J. R. Koe, *J. Am. Chem. Soc.* **2004**, *126*, 13822–13826.
- [11] a) W. Łuzny, E. J. Samuelsen, D. Djurado, Y. F. Nicolau, *Synth. Met.* **1997**, *90*, 19–23; b) J. P. Pouget, C. H. Hsu, A. G. MacDiarmid, A. J. Epstein, *Synth. Met.* **1995**, *69*, 119–120; c) D. Djurado, Y. F. Nicolau, P. Rannou, W. Luzny, E. J. Samuelsen, P. Terech, M. Bee, J. L. Sauvajol, *Synth. Met.* **1999**, *101*, 764–767.
- [12] Z. Wei, T. Laitinen, B. Smarsly, O. Ikkala, C. F. Faul, *J. Angew. Chem.* **2005**, *117*, 761–766; *Angew. Chem. Int. Ed.* **2005**, *44*, 751–756; *Angew. Chem. Int. Ed.* **2005**, *44*, 751–756.
- [13] a) M. Fu, Y. Zhu, R. Tan, G. Q. Shi, *Adv. Mater.* **2001**, *13*, 1874–1877; b) M. Tanaka, R. J. Young, *Biomacromolecules* **2006**, *7*, 2575–2852; c) M. V. Kakade, S. Givens, K. Gardner, K. H. Lee, D. B. Chase, J. F. Rabolt, *J. Am. Chem. Soc.* **2007**, *129*, 2777–2782.
- [14] a) M. Tagowska, B. Palys, K. Jackowska, *Synth. Met.* **2004**, *142*, 223–229; b) M. C. Bernard, A. H. L. Goff, *Synth. Met.* **1997**, *85*, 1145–1146.

Received: April 19, 2010  
Published online: June 25, 2010